Remote Sensing in Ecology and Conservation
Open Access
ZSL LET'S WORK FOR WILDLIFE

ORIGINAL RESEARCH

An innovative use of orthophotos – possibilities to assess plant productivity from colour infrared aerial orthophotos

Rasmus Erlandsson[1], Marianne Stoessel[2], Helle Skånes[2], Marika Wennbom[2] & Anders Angerbjörn[1]

[1]Department of Zoology, Stockholm University, SE-106 91, Stockholm, Sweden
[2]Department of Physical Geography, Stockholm University, SE-106 91, Stockholm, Sweden

Keywords
Aerial photography, habitat modelling, mountain tundra, NDVI, near infrared, primary productivity

Correspondence
Rasmus Erlandsson, Department of Zoology, Stockholm University, SE-106 91 Stockholm, Sweden. Tel: +46 8 16 40 52;
E-mail: rasmus.erlandsson@zoologi.su.se

Editor: Ned Horning
Associate Editor: Jian Zhang

Received: 15 August 2018; Revised: 21 December 2018; Accepted: 9 January 2019

doi: 10.1002/rse2.108

Remote Sensing in Ecology and Conservation 2019;**5** (4):291–301

Abstract

Studies of ecological processes should focus on a relevant spatial scale, as crude spatial resolution will fail to detect small scale variation which is of potentially critical importance. Remote sensing methods based on multispectral satellite images are used to assess primary productivity and aerial photos to map vegetation structure. Both methods are based on the principle that photosynthetically active vegetation has a characteristic spectral signature. Yet they are applied differently due to technical differences. Satellite images are suitable for calculations of vegetation indices, for example Normalized Difference Vegetation Index (NDVI). Colour infrared aerial photography was developed for visual interpretation and never regarded for calculation of indices since the spectrum recorded and post processing differ from satellite images. With digital cameras and improved techniques for generating colour infrared orthophotos, the implications of these differences are uncertain and should be explored. We tested if plant productivity can be assessed using colour infrared aerial orthophotos (0.5 m resolution) by applying the standard NDVI equation. With 112 vegetation samples as ground truth, we evaluated an index that we denote rel-$NDVI_{ortho}$ in two areas of the Fennoscandian mountain tundra. We compared the results with conventional SPOT5 satellite-based NDVI (10 m resolution). rel-$NDVI_{ortho}$ was related to plant productivity (Northern area: $P = <0.001$, $R^2 = 0.73$; Southern area: $P = <0.001$, $R^2 = 0.39$), performed similar to SPOT5 satellite NDVI (Northern area: $P = <0.001$, $R^2 = 0.76$; Southern area: $P = <0.001$, $R^2 = 0.40$) and the two methods were highly correlated (cor = 0.95 and cor = 0.84). Despite different plant composition, the results were consistent between areas. Our results suggest that vegetation indices based on colour infrared aerial orthophotos can be a valuable tool in the remote sensing toolbox, offering a high-spatial resolution proxy for plant productivity with less signal degradation due to atmospheric interference and clouds, compared to satellite images. Further research should aim to investigate if the method is applicable to other ecosystems.

Introduction

Primary productivity of green plants is the foundation of terrestrial food webs and a key factor shaping ecosystems. In many landscape ecological studies, it is therefore crucial to accurately measure or estimate primary productivity at an appropriate scale. The relevant scale of ecological processes, in space and time, is linked to the characteristics of the organisms involved (Wiens 1989). In animal ecology for example, spatial scale is related to body mass, as large animals have disproportionately large home-range sizes (McNab 1963; Jetz et al. 2004), while population density on the other hand is negatively related to body mass (Damuth 1981). For example, small-size herbivores such as insects damaging forests, or lemmings grazing tundra vegetation, can reach numbers where they

affect the vegetation substantially enough to be detected with satellite imagery during population peaks (Vogelmann and Rock 1989; Olofsson et al. 2012). Despite striking regional patterns, however, ecological variation at a local scale might determine the mechanisms behind spatial and temporal dynamics of such organisms. For example, within an individual home range, local habitat and microclimate can offer refugia that are vital to plants and animals in otherwise non-suitable biotopes (Suggitt et al. 2011).

At local scale, a method with too low resolution will reduce the variance in the collected data and fail to detect important small-scale differences (Wiens 1989). Data with high-spatial resolution can therefore become a necessity for mechanistic understanding of ecological processes even at a landscape scale. Surveying vegetation over large areas in the field is, however, both time-consuming and expensive. Remote sensing methods are therefore often used as a complement to field studies to assess vegetation in an efficient and reliable way. Multispectral satellite imagery is the most commonly used source for remote sensing of vegetation (Jones and Vaughan 2010) but also near infrared aerial photos are used for detailed manual surveillance of vegetation (Ihse 2007; Morgan et al. 2010). Both methods are based on the common basic principle that photosynthetically active vegetation has a characteristic spectral signature or reflectance pattern of electromagnetic radiation.

Technical background

The radiometric information recorded by multispectral satellite images is suitable for image transformation and characterization of land cover, and calculation of vegetation indices (Tucker 1979; Bannari et al. 1995; Jones and Vaughan 2010). A wealth of vegetation indices has emerged, and in a review of 40 different types Bannari et al. (1995) found individual advantages justifying the use for certain purposes of each index covered in the study. Those strengths, however, came at the expense of different drawbacks leaving no magic bullet solution. The authors concluded that the choice of index therefore depends on the application (Bannari et al. 1995). A commonly used vegetation index, typically calculated from multispectral satellite images, is the Normalized Difference Vegetation Index (NDVI) that utilizes information in the red and near infrared spectral bands to capture key characteristics in the spectral signature of photosynthetically active vegetation (Rouse 1974; Tucker 1979; Buchhorn et al. 2013).

Multispectral satellite images are available from many different sensors of varying coverage as well as temporal and spatial resolutions. Examples of satellites carrying multispectral sensors are NOAA AVHRR (1.1 km resolution), MODIS (250–1000 m), LANDSAT (30–60 m), SENTINEL 2 (10–60 m) and SPOT (5–20 m). The quality of satellite imagery is constantly improving with better temporal, spectral and/or spatial resolutions, and currently, there are multispectral satellite sensors with a spatial resolution around or below 1 m, for example Worldview-4 (0.31–1.24 m) and SkySat (down to 0.8 m). On the other hand, the satellite images with high-spatial resolution tend to be costly or hard to access. In addition, there is a trade-off between spatial and temporal resolution and/or spatial coverage limiting their usability.

Regardless of their spatial resolution, satellite images are affected by atmospheric effects such as scattering, reflection and absorption of light (Chavez 1996). This will affect the image but can be compensated to some degree through atmospheric correction (Steven et al. 2003). Clouds and their shadows, however, can effectively obscure land cover signals and can only be handled through averaging of measurements based on multiple images from different dates (Ju and Roy 2008; Karlsen et al. 2018). The extent of cloud cover in an area will thus affect the likelihood to obtain suitable images and a high number of images available for an area do not guarantee that any of them will be useful. This means that despite an impressive amount of satellite images available today, there are still areas that are difficult to monitor due to few days with suitable weather. Naturally, longer time series of multispectral images are also limited in those areas. Also, the use of averaged images containing information from different times during the vegetation season might not be suitable for the task at hand.

Another widely used remote sensing technique to study vegetation is colour infrared aerial photography that was developed for visual interpretation of landscape features and not with radiometric transformation in mind (Ihse 2007; Jones and Vaughan 2010; Morgan et al. 2010). These are the precursors of satellite techniques that were developed later. The field of aerial remote sensing is developing quickly as well, with global use of multispectral digital cameras in the last 10 years. Recently, in addition to conventional aeroplanes and their cameras, drone-based sensors are booming for small scale surveys (Anderson and Gaston 2013; Klemas 2015). Small drones offer many benefits as they are versatile, can be fitted with any type of sensor and are cost-effective on a local scale. On a larger scale however, small drones are limited by their relatively short airtime, low fly altitude and the post processing work that would be required for such fine resolution (in cm) applied on large scale (in km). Although drone technology is a promising tool in the field of remote sensing it falls outside the scope of this study.

Colour infrared aerial photos are traditionally acquired by cameras carried on land survey aeroplanes, and in contrast to satellites they are only produced during optimal weather conditions and are less affected by atmospheric interference than satellites due to low flight height. They contain information in the visual and near infrared parts of the electromagnetic spectrum with a high-spatial resolution (in Swedish national campaigns typically 0.25–0.5 m; Lantmäteriet 2013). However, aerial photos are enhanced to facilitate human interpretation which affects the pixel values within the individual picture, and pictures over different areas might be processed in different ways. Furthermore, the cameras' sensitivity span for near infrared radiation is wider than corresponding bands for satellites, and partly overlaps with the red band (Ryan and Pagnutti 2009; Gruber and Prassl 2012; Fig. 1). Consequently, colour infrared aerial photos are conventionally regarded as unfit for image transformation and index calculation and we have not found that they have been used to assess primary productivity before. Still, colour infrared aerial orthophotos are increasingly used to automatically separate vegetation from non-vegetation (Banzhaf and Hofer 2008; Grafius et al. 2016; Beaumont et al. 2017). If it would be possible to use the information contained in the colour infrared aerial photos to obtain some assessment of primary productivity it could provide a fruitful way to investigate vegetation over regional areas of several square km with a high spatial resolution, especially in areas with low-satellite coverage.

Any new method has to be evaluated, primarily using empirical field data. Nonetheless a comparison with well-established standard methods is also of interest as a bench mark of a new or modified method. Despite the obvious shortcomings of aerial photos regarding radiometric accuracy and consistency, the effect of the technical differences in the recorded signal between satellite images and colour infrared aerial photos is not fully investigated and the practical importance remains to be evaluated. For example, which part of the colour infrared spectrum that is used as input data is reported to have little effect on NDVI, in contrast to the width of it (Teillet et al. 1997). In combination with empirical data on primary productivity, a comparison of indices based on satellite images and aerial photos would reveal if the radiometric differences have practical implications or more of a theoretical nature.

Scope of the study

We believe that the potential of colour infrared aerial orthophotos is underestimated if they can be used for calculating vegetation indices achieving ecologically meaningful results with high-spatial resolution in areas with limited satellite imagery coverage, or where more detailed resolution is needed. We consequently transformed high-resolution colour infrared orthophotos, without prior calibration using the standard NDVI equation (Eq. 1) and computed what we denote a *relative Orthophoto Normalized Difference Vegetation Index* (rel-$NDVI_{ortho}$). The name rel-$NDVI_{ortho}$ indicates that the standard NDVI equation was applied on uncalibrated aerial image values (digital numbers) resulting in relative NDVI values as opposed to NDVI values based on calibrated reflectance values from a satellite image. The equation for calculating NDVI using radiometric intensity in the near infrared and red spectrum.

$$\mathrm{NDVI} = \frac{\text{near infrared - red}}{\text{near infrared} + \text{red}} \quad (1)$$

With sampled vegetation as a ground truth, we tested the hypothesis that rel-$NDVI_{ortho}$ can predict plant productivity in a mountain tundra ecosystem. We applied the method in two study areas which were 380 km apart, to see if it was possible to generalize it between different sites within the same biome and using images from different cameras. Finally, we also compared the method to conventional, radiometrically correct, satellite-based NDVI (SPOT 5).

Materials and Methods

Remote sensing and image processing

We computed rel-$NDVI_{ortho}$ with the standard NDVI equation (Eq. 1; Tucker 1979) using pixel values from colour infrared orthophotos provided by the Swedish mapping, cadastral and land registration authority *Lantmäteriet*. The data were resampled to 2 m from the original 0.5 m resolution to match the precision of our satellite navigation units and to reduce computational workload (Fig. 3). The orthophotos were derived from images taken with two different cameras, *VEXCEL UltraCam Eagle* in the Northern area and *Z/I Imaging DMC* in the Southern area (for further details see supplementary information). $NDVI_{SPOT5}$ was computed using SPOT 5 satellite images (10 m resolution). SPOT 5 images were corrected for atmospheric noise using the *Quick Atmospheric Correction* (QUAC) method (Bernstein et al. 2005, 2006). We resampled images with higher resolution (orthophoto) to 10 m resolution to allow a valid comparison of different sources in some of the analyses. Resampling was done in Quantum GIS 2.2.0 (QGIS Development Team 2009). In the Northern area, the SPOT 5 images (2015-08-18) and the aerial photos (2015-09-03) were acquired within 16 days. In the Southern area, the dates of the images used were 11 days apart but

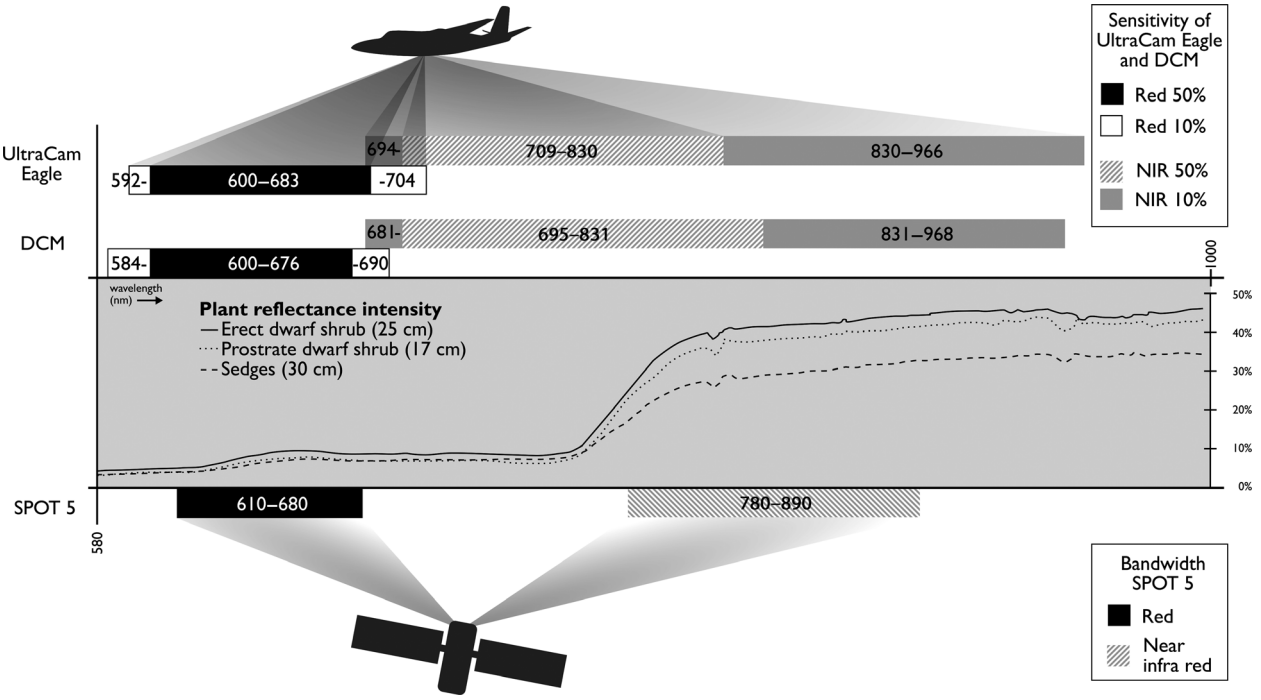

Figure 1. The sensitivity in the spectrums used for calculation of NDVI of the sensors covered in the study. DCM cam and UltraCam Eagle are used for production of orthophotos. They are similar to each other but differ from SPOT5 regarding the bandwidth in the near infrared (NIR) spectrum. Percentage indicates thresholds where the signal reaches above 50% and 10% of the peak sensitivity. Curves show reflectance intensity, a spectral signature, for different functional vegetation groups (shrubs and sedges) in low-arctic tundra (adaptation from Buchhorn et al. 2013).

from different years (SPOT 5: 2014-07-13, Orthophotos: 2008-07-24).

Study areas

We worked in two areas in Sweden, 380 km apart (Fig. 2). The *Northern area*: in the vicinity of mount *Äivisåive* (1250 m a.s.l., N 65°54′, E 16°03′*)*, *Vindelfjällen*, county of Västerbotten, the 8–10 of August 2016 (Fig. 2). The *Southern area*: around mount *Helags* (1796 m a.s.l., N 62°54′, E 12°27′), county of Jämtland, the 2–5 of September 2014. Both areas consist of mountain tundra above the tree line (800–900 m.a.s.l.), comprising dry heaths, grass heaths, meadows, fens and lakes (Ulfstedt 1977; Borgström 1979). Snow cover normally (averages for 1961–1990) lasts from October to early June (Swedish Meteorological and Hydrological Institute 2016).

The Scandinavian mountain tundra hosts a limited number of vascular plant species. There are slow long-term changes in vegetation but large intra-regional contrasts in growing conditions due to altitude, slope and aspect. The between-year variation in weather, affecting for example snow melting, can have a large impact on the start of the growing season and hence on the vegetation. However, none of the years involved in the study showed any particular meteorological anomalies, and we are confident that the sampled vegetation in August and September is a representative of the peak standing crop biomass in the system.

Vegetation ranges from lush and dense to meagre and non-existent depending on different edaphic and climatic conditions. The hilly terrain of the mountain tundra also allows for sampling at different altitudes and of slopes with different aspects while still being covered by colour infrared orthophotos processed in a consistent way.

Sampling of vegetation

We sampled vegetation in our two study areas using a stratified random sampling design throughout the landscape with different combinations of rel-$NDVI_{ortho}$ values, altitude, aspect and slope (Fig. 2). No data points were located in shadows. The plots were located in the field using hand held GPS+GLONASS satellite navigation units (Garmin eTrex 10), when the unit stated a maximum deviance of 2 m.

For each plot (1 × 1 m square), we collected all above-ground vegetation in paper bags from three

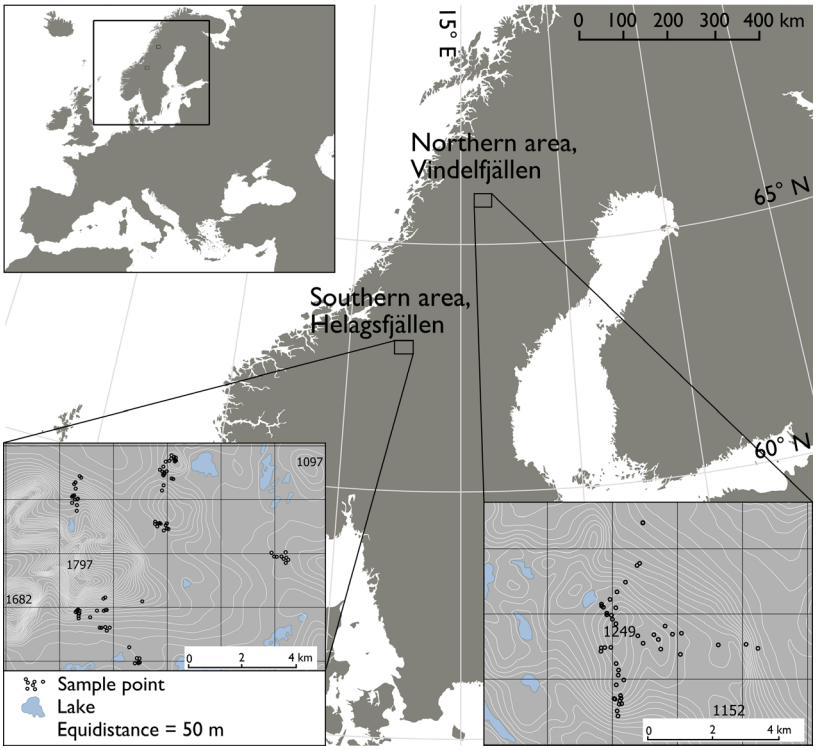

Figure 2. The location of the two sampling sites in Vindelfjällen and Helagsfjällen, Sweden, referred to as the Northern and the Southern area.

randomized quadrats (0.2 × 0.2 m) and pre-dried them the same afternoon in order to halt decomposition (Fig. 3). We brought the pre-dried samples to a laboratory and sorted them into four functional groups: (I) yearly crop of shrubs and sprigs, (II) twigs and needles, (III) graminoids, (IV) herbs. Roots, mosses and dead vegetation litter were removed from the samples. Prior to weighing, we dried the samples at 70°C for at least 24 h, or until completely dry. We weighed samples using a digital scale KERN PCB100-3 (±0.001 g). The sampled green biomass is here after denoted *plant productivity* (following Karlsen et al. 2018). A direct relationship between net primary productivity and plant biomass can be assumed for yearly crop of shrubs and sprigs, graminoids and herbs although it is usually an underestimate (Singh et al. 1975). It was, however, not possible to distinguish the current yearly crop of twigs and needles from previous years, so some amount of the sampled twigs and needles biomass originates from previous years production.

Statistical analysis

We fitted two linear regression models for each area with the logarithm of plant biomass as explanatory variable and rel-$NDVI_{ortho}$ respectively $NDVI_{SPOT5}$ as response variable. To allow logarithms of zero values, 1 was added to all biomass measurements. To compare the different index values with each other, we calculated correlation coefficients for NDVI and rel-$NDVI_{ortho}$ values of each plot, and tested the correlations for significance. All measurements were carried out in the statistical software R 3.1.2 (R Core Team 2014; packages: CAR (Fox and Weisberg 2011)).

Results

We collected 112 vegetation samples ($n_{Northern} = 46$, $n_{Southern} = 66$). The weight of sampled vegetation ranged from 0 to 29.19 g in the Northern area and 0–164 g in the Southern area. The densest vegetation was found in wet and semi-wet heath biotopes covered by graminoids and small woody plants such as dwarf birch (*Betula nana* L.), juniper (*Juniperus communis* L.) and woolly willow (*Salix lanata* L.). The scarcest vegetation was in stony areas with lichens but no vascular plants.

Our hypothesis was supported as rel-$NDVI_{ortho}$ increased with biomass and hence reflected plant productivity (Fig. 4). The explained variation was $R^2 = 0.73$ ($n = 44$, d.f. = 1, $P < 0.001$) in the Northern area and $R^2 = 0.39$ ($n = 66$, d.f. = 1, $P < 0.001$) in the Southern area. This was similar to the relationship between biomass and $NDVI_{SPOT5}$ where the explained variation was

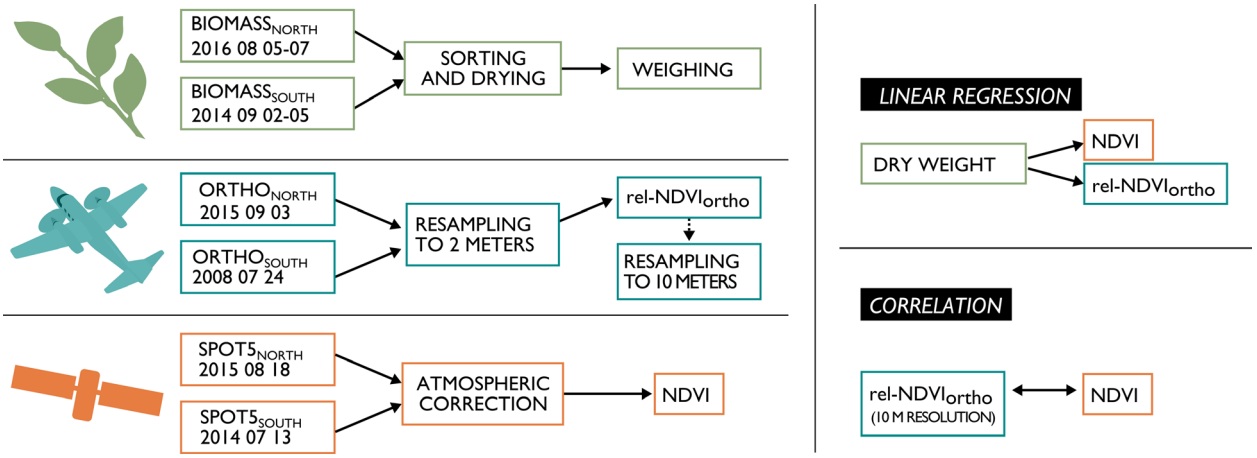

Figure 3. Flow chart over the procedures and analyses used in the study.

$R^2 = 0.76$ ($n = 46$, d.f. = 1, $P < 0.001$) in the Northern area and $R^2 = 0.40$ ($n = 66$, d.f. = 1, $P < 0.001$) in the Southern area (Fig. 4).

To compare the two methods, rel-$NDVI_{ortho}$ and $NDVI_{SPOT5}$, we tested if the slopes of the two regression lines in each area differed from each other. A linear regression with an interaction term was fitted and showed no significant difference ($P_{Southern} = 0.81$; $P_{Northern} = 0.075$). In both areas, the range of rel-$NDVI_{ortho}$ values seemed to consistently turn out roughly 0.55 lower than the corresponding $NDVI_{SPOT5}$ values (Fig. 4, Fig. 5). The $NDVI_{SPOT5}$ and rel-NDVIortho (resampled to 10 m) were highly correlated with each other and with plant productivity in both areas (Northern area: cor = 0.95, confidence

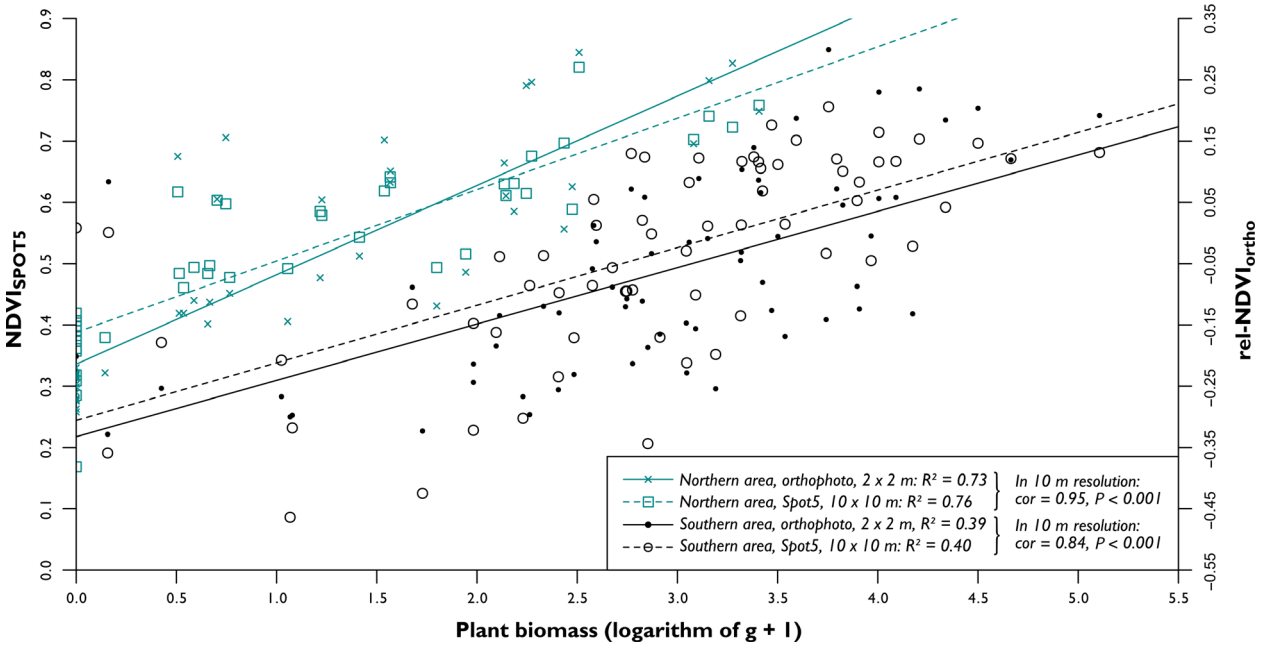

Figure 4. Biomass explained rel-$NDVI_{ortho}$ (based on near infrared orthophotos). A similar relationship was found using $NDVI_{SPOT5}$ (based on SPOT5 satellite images), and the two methods were highly correlated (cor = 0.95 in the Northern area, cor = 0.84 in the Southern area). The variance explained was similar for the two methods but differed between the two areas. Northern area: $NDVI_{SPOT5}$: $R^2 = 0.76$ ($n = 46$, $P < 0.001$), rel-$NDVI_{ortho}$: $R^2 = 0.73$ ($n = 46$, $P < 0.001$). In the Southern area: $NDVI_{SPOT5}$: $R^2 = 0.40$ ($n = 66$, $P < 0.001$), rel-$NDVI_{ortho}$: $R^2 = 0.39$ ($n = 66$, $P < 0.001$). The slopes of the lines did not differ from each other (Northern area: 0.075, Southern area: 0.81). The rel-$NDVI_{ortho}$ is plotted on the right y-scale, 0.55 lower than the $NDVI_{SPOT5}$.

interval = 0.91–0.97, $P < 0.001$; Southern area: cor = 0.84, CI = 0.74–0.90, $P < 0.001$; Figs. 4 and 5).

Discussion

Plant productivity was successfully detected by rel-$NDVI_{ortho}$ in both study areas. The results showed that despite temporal and radiometric differences, the correlation between conventional $NDVI_{SPOT5}$ and rel-$NDVI_{ortho}$ was high, except that rel-$NDVI_{ortho}$ appeared to be consistently around 0.55 lower than the NDVI values in both areas (Figs. 4 and 5). The shift was linear over the range of plant productivity and similar in the two areas, indicating that this difference in NDVI values holds no direct ecological value. Our two study sites were separated in both time and space and the index was based on images from two different cameras, which supports that this constant could be generalized within mountain tundra ecosystems. We therefore suggest that rel-$NDVI_{ortho}$ could be evaluated relative to NDVI through a calibration, sliding the two indices into position by adding a constant to rel-$NDVI_{ortho}$ (Fig. 4). The lower values of the rel-$NDVI_{ortho}$ could be related to the broader sensitivity of the sensors used for colour infrared orthophotos. Bandwidths of 30 nm are optimal for calculating NDVI and wider bandwidths are known to render false low index values that drop down to −0.15 when bandwidths reach 50–150 nm (Teillet et al. 1997). For UltraCam Eagle, the bandwidth of the red spectrum is *c.* 112 nm and around 270 nm in the near infrared spectrum and DMC has a similar specification (Fig. 1). However, the lower-index values could be useful. Saturation, where the NDVI values in high-photosynthesizing environments tend to reach the maximum value of 1, is a well-known problem when calculating NDVI in areas with very dense vegetation (Sellers 1985; Mutanga and Skidmore 2004). Although the mountain tundra does not contain any highly productive areas and we could not test it, a rel-$NDVI_{ortho}$ less sensitive to saturation could provide a more detailed scale and improve the ability to separate differences in highly productive environments.

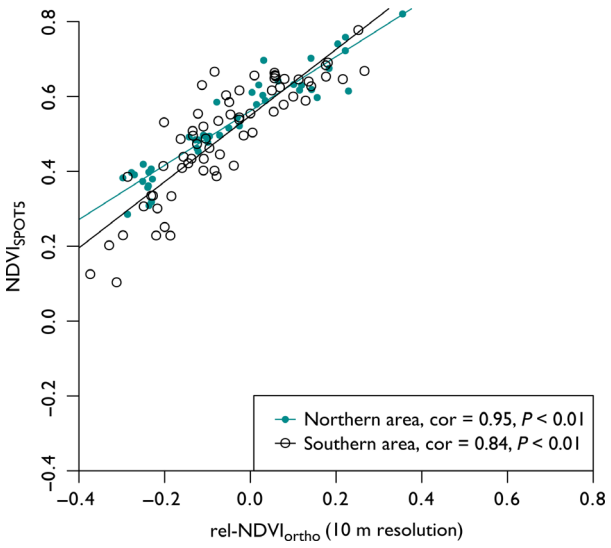

Figure 5. The values of $NDVI_{SPOT5}$ and rel-$NDVI_{ortho}$ plotted against each other. The rel-$NDVI_{ortho}$ had values shifted about -0.55 compared with conventional satellite-based NDVI.

The correlation between rel-$NDVI_{ortho}$ values and $NDVI_{SPOT5}$ was strong and consistent despite the different treatment of the original data (Fig. 5). Orthophotos go through post processing that impairs their absolute pixel value accuracy compared to satellite images, which commonly go through correction procedures compensating for effects such as atmospheric distortion and local solar zenith angle to assess a true earth surface reflectance. The pixel values of orthophotos can therefore not be directly compared with corrected radiometric data from satellite imagery, and possibly account for the −0.55 shift to some extent. Although this could be considered a limitation, we do believe that this is an important aspect of our study showing that digital numbers can give relevant information on the plant productivity and not only an indication of the density of the vegetation cover in general. This opens up for users that are not skilled remote sensing technicians or wish to work with easily available high-resolution data that are not satellite imagery. We show that images provided by professional image providers, where the level of processing is sometimes not well-documented, can be used without further image processing. The lack of absolute radiometric accuracy should also be seen in the light of the lesser atmospheric noise for aerial photos, consistent photo conditions and the substantially increased spatial resolution. The near infrared bandwidth of the aerial photo cameras is rather wide, yet the maximum sensitivity is in a shorter wavelength compared to SPOT5, and shorter wavelengths of the infrared band are less affected by water evaporation (Teillet et al. 1997). A potentially lower sensitivity together with the closer distance between lens and landscape feature could therefore produce a less distorted signal in aerial orthophotos thereby reducing the need for atmospheric corrections, and potentially counterbalancing some of the inaccuracies caused by manual manipulation in the post processing of the aerial photos.

In an investigation of how bandwidths of different satellites affect NDVI, Teillet et al. (1997) showed that the sensitivity of a sensor also affects other indices similar to NDVI (e.g. SAVI, MSAVI and DVI). The potential of radiometric information in colour infrared orthophotos, demonstrated by our results, suggests that orthophotos

might be useful for the calculation of other indices that also make use of the relationship between the red and near infrared parts of the electromagnetic spectrum.

For both methods, the model intercept in the Northern area appeared to be higher than the intercept in the Southern area. This is possibly a reflection of the sampled vegetation types and the range of biomass sampled. In the Northern area, the samples weighed 0–29 g and consisted to a large proportion of graminoids and herbs while they in the Southern area ranged from 0 to 164 g and were dominated by shrubs and sprigs (Fig. 6). The yearly crop of graminoids and herbs has a high-photosynthetic activity and hence a proportionally high NDVI per biomass. The yearly crop of a shrub on the other hand consists to a larger extent of woody parts that are less photosynthetically active and would render a lower index value per biomass. The images used in the Northern area were also taken later in the season which could explain some of the difference in intercept between the two areas. Seasonal timing of imaging is important as the remote sensing of plant productivity has to be done during peak standing crop biomass. Additionally, the inclination of sunlight affects which features are shaded or visible to the sensor, which in turn affects the radiometric signal during the day (Huete 1987; Galvão et al. 2004). The strength of aerial photos is that they typically are taken at a similar time of the day and during optimal weather conditions, thereby limiting the effects of differences in timing. Such consistency can be harder to obtain with those satellites that have a limited revisiting frequency, but timing is an inevitable problem for all remote sensing methods.

Although we resampled orthophotos of 0.5 m resolution to 2 m for the analyses, we see no reason to believe that the method would perform less well in the original resolution, suggesting that, even though we did not test their original resolution, orthophotos could provide a basis for vegetation indices calculated with a high-geometrical resolution and good accuracy at a limited cost.

The resolution of the aerial photos was reduced to 2 × 2 m to match the precision of our satellite navigation units that did not allow us to perfectly align each 1 × 1 m plot with corresponding aerial photo pixel. Reduced resolution is known to result in scale-dependent errors, as small-scale heterogeneity inevitably is lost during resampling (Moody and Woodcock 1994). However, samples were mostly collected in homogeneous vegetation where the sampled 1 × 1 m plots were representative of the corresponding 10 × 10 m area, limiting potential effects of navigational error and vegetation heterogeneity (similarly to Karlsen et al. 2018). We therefore believe that the precision of our ground truth corresponding to pixel values was good enough to reliably address and test our hypothesis regarding orthophotos. The strong

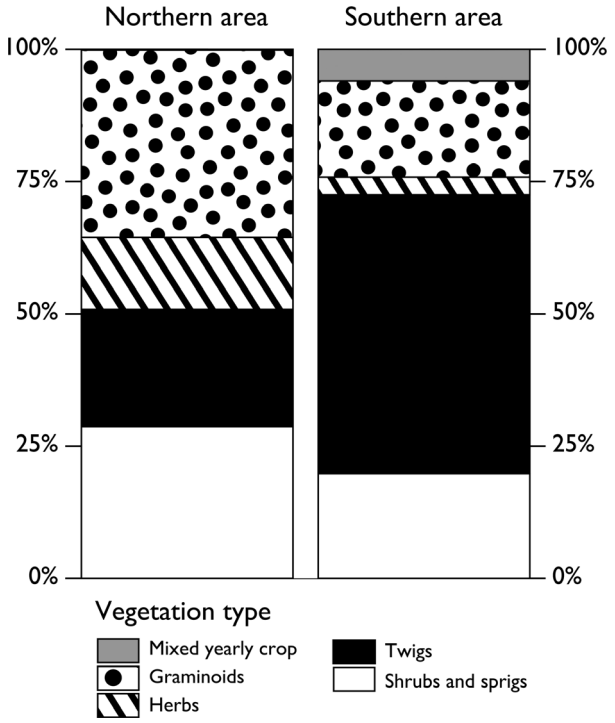

Figure 6. Composition of sampled vegetation in proportion of total collected material. The material collected in the Northern area (n = 46, weight range = 0–29 g) was dominated by annuals while the samples in the Southern area (n = 57, weight range = 0–164 g) were dominated by shrubs and sprigs.

similarities between the both methods also suggest that the resampling of orthophotos to match the 10 m SPOT resolution did not have any major implications. Yet we cannot rule out an effect of small scale vegetation heterogeneity and the limited possibility to perfectly align our data. Such an effect would increase the unexplained variation and could possibly explain the lower R^2 value in the Southern area, as the sampled vegetation there was more heterogeneous in general.

The pronounced similarities between rel-$NDVI_{ortho}$ and $NDVI_{SPOT5}$ in both study areas show that the two approaches performed consistently and that it was possible to apply rel-$NDVI_{ortho}$ across the sampled landscapes. Yet, since we focused solely on a mountain tundra ecosystem, our study is limited and further investigation is needed to test if, for example, the size of the relative shift in index values compared to NDVI is consistent for different types of plant communities or whether it is ecosystem specific. Even if a shift would differ between ecosystems, this would be less of a problem as long as it remains linear. If so, control points of the rel-$NDVI_{ortho}$ would only need to be calibrated with a satellite image before being applied on its own merits.

The usability of rel-$NDVI_{ortho}$ suggests that there is a potential for research projects to tailor future high-resolution monitoring at a moderate expense using standard land survey aeroplanes. This could be a valuable addition to traditional satellite images as a proxy for radiometric information in areas where satellite images do not achieve the spatial or (due to cloud cover) temporal resolution needed; or the main method if the operational scale of a target organism group requires a resolution higher than 10–30 m. If the photogrammetric camera technique would evolve to facilitate radiometric computation, that is if the number of bands in cameras used for aerial photography would increase, allowing narrower bands with less or no spectral overlap in the near infrared spectrum, and perhaps add a band in the red edge, the usage of colour infrared aerial photography would be greatly improved. Small remote sensing drones fitted with multispectral sensors is another way to achieve high-resolution surveys of vegetation that has already been proven useful (Anderson and Gaston 2013; Klemas 2015). The practicality of such systems will however likely remain limited to local studies as they will meet both technical and economic challenges on a regional scale compared to aerial photos. Colour infrared aerial orthophotos therefore appear to provide an interesting high-resolution method that has a place between large-scale satellites and highly localized small drones.

We have applied rel-$NDVI_{ortho}$ in a number of recent studies where it has been shown to be useful in modelling lemming abundance on a 5–30 m scale (Le Vaillant et al. 2018) and in modelling species interactions within the terrestrial arctic predator guild (Stoessel et al. 2018) in mountain tundra ecosystems. But also in biotope mapping in urban and rural landscapes, rel-$NDVI_{ortho}$ has shown to be useful to automatically separate vegetation covered land from non-vegetation, which is a highly desirable separation, even without the attempt to translate rel-$NDVI_{ortho}$ values into an estimation of primary productivity (Akbari et al. 2003; Grafius et al. 2016; Skånes and Stoessel 2016).

Concluding remarks

We found support for our hypothesis that it was possible to reliably assess plant productivity in the mountain tundra at a very fine spatial scale by transforming colour infrared aerial orthophotos using the algorithm for NDVI; resulting in rel-$NDVI_{ortho}$. Using satellite-based NDVI, we establish a relationship between our new application and the widely used standard method. However, the shift in absolute index values highlights the relative characteristics of rel-$NDVI_{ortho}$. Our results open up new possibilities for the use of digital colour infrared orthophotos as a basis for image transformation, revealing an increased potential use for the vast number of available digital aerial photos with their high-image quality, low distortion and high (<1 m)-spatial resolution.

Given our results, we can conclude that rel-$NDVI_{ortho}$ can be used as a proxy of plant productivity that has a good potential to drastically improve the usability of colour infrared orthophotos in mountainous areas, and as such contribute to the use of remote sensing for small scale ecological processes in plant, animal and landscape ecology while retaining a regional perspective, complementing the use of satellite images and small drone imagery.

Acknowledgments

The authors would like to thank S. Menci for assisting in the laboratory, fieldworkers who helped to collect samples, personnel at Lantmäteriet for technical support, M. Parsons and A. Kahrl for language proofing and E. Zachariassen for inspiration. The Swedish Tourist Association (*Svenska turistföreningen*) was helpful in storing of samples. We are also grateful for the comments from two anonymous reviewers that helped to improve the manuscript. The salary of R. Erlandsson was financed by Fjällräven International AB. The study was partly financed by EU/Interreg Sweden-Norway Felles Fjellrev II (Project-id: 20200939).

References

Akbari, H., L. S. Rose, and H. Taha. 2003. Analyzing the land cover of an urban environment using high-resolution orthophotos. *Landsc. Urban Plan.* **63**, 1–14.

Anderson, K., and K. J. Gaston. 2013. Lightweight unmanned aerial vehicles will revolutionize spatial ecology. *Front. Ecol. Environ.* **11**, 138–146. https://doi.org/10.1890/120150.

Bannari, A., D. Morin, F. Bonn, and A. R. Huete. 1995. A review of vegetation indices. *Remote Sens. Rev.* **13**, 95–120. https://doi.org/10.1080/02757259509532298.

Banzhaf, E., and R. Hofer. 2008. Monitoring urban structure types as spatial indicators with CIR Aerial photographs for a more effective urban environmental management. *IEEE J. Sel. Top. Appl. Earth Obs. Remote Sens.* **1**, 129–138. https://doi.org/10.1109/jstars.2008.2003310.

Beaumont, B., T. Grippa, M. Lennert, S. Vanhuysse, N. Stephenne, and E. Wolff. 2017. Toward an operational framework for fine-scale urban land-cover mapping in Wallonia using submeter remote sensing and ancillary vector data. *J. Appl. Remote Sens.* **11**, 1. https://doi.org/10.1117/1.JRS.11.036011.

Bernstein, L., S. Adler-Golden, R. Sundberg, R. Levine, T. Perkins, A. Berk, et al. 2005. Validation of the QUick Atmospheric Correction (QUAC) algorithm for VNIR-SWIR

multi-and hyperspectral imagery. Pp. 668–678 in Proceedings volume 5806, Algorithms and Technologies for Multispectral, Hyperspectral, and Ultraspectral Imagery XI. International Society for Optics and Photonics. https://doi.org/10.1117/12.603359

Bernstein, L., S. Adler-Golden, R. Sundberg, and A. Ratkowski. 2006. Improved reflectance retrieval from hyper-and multispectral imagery without prior scene or sensor information. P. 63622 *in* Proceedings volume 6362, Remote Sensing of Clouds and the Atmosphere XI. International Society for Optics and Photonics.

Borgström, I. 1979. *Geomorphological map 18 C Sylarna: description and assessment of areas of geomorphological importance*. Statens naturvårdsverk, Solna.

Buchhorn, M., D. Walker, B. Heim, M. Raynolds, H. Epstein, and M. Schwieder. 2013. Ground-based hyperspectral characterization of Alaska tundra vegetation along environmental gradients. *Remote Sens.* **5**, 3971–4005. https://doi.org/10.3390/rs5083971.

Chavez, P. S. 1996. Image-based atmospheric corrections-revisited and improved. *Photogramm. Eng. Remote Sens.* **62**, 1025–1035.

Damuth, J. 1981. Population density and body size in mammals. *Nature* **290**, 699–700.

Fox, J., and S. Weisberg. 2011. *An R companion to applied regression*. Sage, Thousand Oaks CA.

Galvão, L. S., F. J. Ponzoni, J. C. N. Epiphanio, B. F. T. Rudorff, and A. R. Formaggio. 2004. Sun and view angle effects on NDVI determination of land cover types in the Brazilian Amazon region with hyperspectral data. *Int. J. Remote Sens.* **25**, 1861–1879. https://doi.org/10.1080/01431160310001598908.

Grafius, D. R., R. Corstanje, P. H. Warren, K. L. Evans, S. Hancock, and J. A. Harris. 2016. The impact of land use/land cover scale on modelling urban ecosystem services. *Landsc. Ecol.* **31**, 1509–1522.

Gruber, M., and P. Prassl. 2012. Calibration report Ultracam Eagle (short version). Graz.

Huete, A. R. 1987. Soil and Sun angle interactions on partial canopy spectra. *Int. J. Remote Sens.* **8**, 1307–1317. https://doi.org/10.1080/01431168708954776.

Ihse, M. 2007. Colour infrared aerial photography as a tool for vegetation mapping and change detection in environmental studies of Nordic ecosystems: a review. *Nor. Geogr. Tidsskr. - Nor. J. Geogr.* **61**, 170–191. https://doi.org/10.1080/00291950701709317

Jetz, W., C. Carbone, J. Fulford, and J. H. Brown. 2004. The scaling of animal space use. *Science* **306**, 266–268.

Jones, H. G., and R. A. Vaughan. 2010. *Remote sensing of vegetation: principles, techniques, and applications*. Oxford University Press, Oxford.

Ju, J., and D. P. Roy. 2008. The availability of cloud-free Landsat ETM+ data over the conterminous United States and globally. *Remote Sens. Environ.* **112**, 1196–1211. https://doi.org/10.1016/j.rse.2007.08.011.

Karlsen, S. R., H. B. Anderson, R. van der Wal, and B. B. Hansen. 2018. A new NDVI measure that overcomes data sparsity in cloud-covered regions predicts annual variation in ground-based estimates of high arctic plant productivity. *Environ. Res. Lett.* **13**, 025011. https://doi.org/10.1088/1748-9326/aa9f75.

Klemas, V. V. 2015. Coastal and environmental remote sensing from unmanned aerial vehicles: an overview. *J. Coast. Res.* **315**, 1260–1267. https://doi.org/10.2112/JCOASTRES-D-15-00005.1.

Lantmäteriet. 2013. Produktbeskrivning: Digitala flygbilder. Available from https://www.lantmateriet.se/globalassets/kartor-och-geografisk-information/flyg–och-satellitbilder/dig_flygb.pdf.

Le Vaillant, M., R. Erlandsson, B. Elmhagen, B. Hörnfeldt, N. E. Eide, and A. Angerbjörn. 2018. Spatial distribution in Norwegian lemming Lemmus lemmus in relation to the phase of the cycle. *Polar Biol.* **41**, 1391–1403. https://doi.org/10.1007/s00300-018-2293-6.

McNab, B. K. 1963. Bioenergetics and the determination of home range size. *Am. Nat.* **97**, 133–140.

Moody, A., and C. Woodcock. 1994. Scale-dependent errors in the estimation of land-cover proportions: implications for global land-cover datasets. *Photogramm. Eng. Remote Sens.* **60**, 585–594.

Morgan, J. L., S. E. Gergel, and N. C. Coops. 2010. Aerial photography: a rapidly evolving tool for ecological management. *Bioscience* **60**, 47–59. https://doi.org/10.1525/bio.2010.60.1.9.

Mutanga, O., and A. K. Skidmore. 2004. Narrow band vegetation indices overcome the saturation problem in biomass estimation. *Int. J. Remote Sens.* **25**, 3999–4014. https://doi.org/10.1080/01431160310001654923.

Olofsson, J., H. Tømmervik, and T. V. Callaghan. 2012. Vole and lemming activity observed from space. *Nat. Clim. Change* **2**, 880–883. https://doi.org/10.1038/nclimate1537.

QGIS Development Team. 2009. *QGIS geographic information system*. Open Source Geospatial Foundation, Beaverton. Available from http://qgis.osgeo.org.

R Core Team. 2014. *R: a language and environment for statistical computing*.R Foundation for Statistical Computing, Vienna, Austria. Available from http://www.R-project.org/

Rouse, J. 1974. Monitoring the vernal advancement and retrogradation (green wave effect) of natural vegetation.

Ryan, R., and M. Pagnutti. 2009. Enhanced absolute and relative radiometric calibration for digital aerial cameras. in D. Fritsch, ed. *Photogrammetric week '09*. Wichmann, Heidelberg.

Sellers, P. J. 1985. Canopy reflectance, photosynthesis and transpiration. *Int. J. Remote Sens.* **6**, 1335–1372. https://doi.org/10.1080/01431168508948283.

Singh, J. S., W. K. Lauenroth, and R. K. Steinhorst. 1975. Review and assessment of various techniques for estimating net aerial primary production in grasslands from harvest data. *Bot. Rev.* **41**, 181–232. https://doi.org/10.1007/BF02860829.

Skånes, H., and M. Stoessel. 2016. *Building a hybrid Biotope database method for Stockholm County: from utopia to the real world - Conference abstract*. The University of Reading, Reading, UK.

Steven, M. D., T. J. Malthus, F. Baret, H. Xu, and M. J. Chopping. 2003. Intercalibration of vegetation indices from different sensor systems. *Remote Sens. Environ.* **88**, 412–422. https://doi.org/10.1016/j.rse.2003.08.010.

Stoessel, M., B. Elmhagen, M. Vinka, P. Hellström, and A. Angerbjörn. 2018. The fluctuating world of a tundra predator guild: bottom-up constraints overrule top-down species interactions in winter. *Ecography* **42**, 1–12. https://doi.org/10.1111/ecog.03984

Suggitt, A. J., P. K. Gillingham, J. K. Hill, B. Huntley, W. E. Kunin, D. B. Roy, et al. 2011. Habitat microclimates drive fine-scale variation in extreme temperatures. *Oikos* **120**, 1–8. https://doi.org/10.1111/j.1600-0706.2010.18270.x.

Swedish Meteorological and Hydrological Institute, S. 2016. Snötäckets utbredning och varaktighet. Available from http://www.smhi.se/kunskapsbanken/meteorologi/snotackets-utbredning-och-varaktighet-1.6323 [accessed 17 October 2016].

Teillet, P., K. Staenz, and D. William. 1997. Effects of spectral, spatial, and radiometric characteristics on remote sensing vegetation indices of forested regions. *Remote Sens. Environ.* **61**, 139–149.

Tucker, C. J. 1979. Red and photographic infrared linear combinations for monitoring vegetation. *Remote Sens. Environ.* **8**, 127–150.

Ulfstedt, A.-C. 1977. *Geomorfologiska kartbladet 25 G Ammarnäs: beskrivning och naturvärdesbedömning*. Statens naturvårdsverk, Solna.

Vogelmann, J. E., and B. N. Rock. 1989. Use of Thematic Mapper data for the detection of forest damage caused by the pear thrips. *Remote Sens. Environ.* **30**, 217–225.

Wiens, J. A. 1989. Spatial Scaling in Ecology. *Funct. Ecol.* **3**, 385–397. https://doi.org/10.2307/2389612.

Supporting Information

Additional supporting information may be found online in the Supporting Information section at the end of the article.

Table S1. Comparison between different airborne remote sensing sensors.

